SYLWESTER KANIA[1,2]**, BARBARA KOŚCIELNIAK-MUCHA**[2]**,
JANUSZ KULINSKI**[2,3]**, PIOTR SŁOMA**[2]

[1]Institute of Physics, Lodz University of Technology, ul. Wólczańska 219,
93-005, Łódź, Poland
[2]Centre of Mathematics and Physics, Lodz University of Technology,
Al. Politechniki 11, 90-924 Łódź, Poland
[3]The Faculty of Mathematics and Natural Sciences, Jan Długosz University
in Częstochowa, Al. Armii Krajowej 13/15, 42-218 Częstochowa, Poland

EFFECT OF MOLECULE DIPOLE MOMENT ON HOLE CONDUCTIVITY OF POLYCRYSTALLINE ANTHRONE AND ANTHRACHINONE LAYERS

Complex analyzes were made using methods of molecular quantum mechanics to investigate the effect of the dipole moment of the molecule carrier drift mobility in polycrystalline layers composed of anthrone and anthrachinone molecules. The differences in the measured mobility values seems to be originated in the variations of the geometry of the frontier orbitals rather than the differences inherent in the crystal arrangement of these molecules, which after all, for both are nearly identical.

Keywords: polycrystalline films, quasi amorphous films, amorphous films, anthrone, anthrachinone, hole drift mobility, carrier transport, TD-DFT.

1. INTRODUCTION

Understanding of the carrier transport in organic materials remains a current research topic since the well-known theories can only partly explain the experimental findings. In particular, many attempts have been done to determine the factors affecting the value of hole and electron mobility in thin films of non-ordered organic polycyclic materials. Defining the scope of the research field associated with this topic leads to the hypothesis that there is a correlation between the shape of the molecule determined by electrostatic potential

isosurface and the mobility value measured in non-ordered layer. In such an approach an intriguing problem is not only the steric hindrance but always the subtle problem of the factors activating the conductivity due to the geometrical factors among which important is appearance of the asymmetry of electron density in the molecule. The only groups compatible with a dipole moment are C_1, C_n, $C_{\infty v}$, C_{nv} and C_s. In molecules belonging to C_n or C_{nv} the permanent dipole must lie along the axis of rotation, and the magnitude depends on the atoms, ion pairs and bond dipoles.

Problem of shaping the geometric structures of a molecules and the geometry of their interactions in the purpose to obtain the higher mobilities [1] is typical for molecular engineering [2]. The problem of the influence of the dipole moment of the molecule on the mobility of charge carriers in a solid phase requires a comparative study of two compounds made of similar molecules forming a similar crystalline solid phase but with varying values of dipole moment of the individual molecules. Calibrating compounds predestined for such studies are anthrone and 1,9-anthrachinone built of the molecules with very similar shape, but with different dipole moment. Both mentioned above compounds crystallize in the nearly identical crystal lattices [3], monoclinic with space group C_{2h}^5 (P2$_1$/a) with bimolecular unit of the dimensions (at room temperature) $a_0 = 15{,}8$ Å, $b_0 = 3{,}94 - 3{,}99$ Å, $c_0 = 7{,}865(10)$ Å, $\beta = 102°43(2)'$ for anthrachinone, and $a_0 = (15.80\pm0.03)$ Å, $b_0 = (3.998\pm0.005)$ Å, $c_0 = (7.86\pm0.16)$ Å, $\beta = 101°\ 40'$ for anthrone [4]. The main difference essential for the reason of this paper is the fact that the anthrachinone molecules being centrosymmetric possess small dipole moment, near zero, opposite to the non-centrosymmetric anthrone molecules which are characterised by large dipole moment of $3{,}5$ D $(1{,}19\cdot10^{-29}$ Cm) (in benzene) [5]. X-ray determination of the structure of anthrone is hindered, the reason is in the fact that orientation of the molecules in the unit cell is arranged statistically (determined with the direction and sense of dipole moment vector strictly correlated with the position of the oxygen atom). So solid anthrone possess higher symmetry than that would be normally expected to two asymmetric molecules present in the unit cell. Refinement obtained from X-ray measurements crystal structure on the planes (100) and (001) is poor and in the X-ray examination the diffuse layers are registered [6]. In the row of molecules parallel to [010] direction, molecules alternate regularly their direction and sense of dipole moment (correlated with the position of oxygen atom). This orientational disorder in crystalline anthrone may be estimated with use of Ising coupling parameter, means as the change in the interaction energy of a pair of molecules invert through theirs centres of mass. This parameter calculated from the intermolecular potential (in the range of 1 kJ mol^{-1}) arises in 90% from the electrostatic interaction between carbonyl

dipoles [7]. These calculations are in good correlation with diffuse scattering observed in the X-ray in the ranges of 1,6±0,1 nm in the *a* direction, 3,6 ±0,9 nm in *b* and 2,5±0,2 nm in *c*. This orientation - inversion disordering further reduces the correlation length in translational symmetry.

To demonstrate, the possibility of a direct correlation between the electronic structure of the molecule and the mobility w carriers it was used quantum mechanical calculations. Such calculations are useful for determining conditions favourable for charge migration. For the practical implementation of the calculation we have used the most prominent methods for calculating excited states, time-dependent density functional theory (TD-DFT) – an extension of density functional theory (DFT). The main reason to exploit TD-DFT is presence of time-dependent potentials produced by electric field in our experiments on conductivity in the layers. In TD-DFT external time-dependent potentials such as electromagnetic waves can be considered as a weak perturbation. Using this method, the dynamic process such as transition between two eigenstates can be described [8]. TD-DFT enable extraction the information about excitation energies, frequency-dependent response properties and photo absorption spectra of the studied molecule. For the polycyclic organics TD-DFT is compromise between accuracy and computational performance.

2. EXPERIMENTAL AND RESULTS

2.1. Experiment

The drift mobility for hole was determined for the layers of anthrone and anthrachinone with use of time of flight method (TOF) exactly in the same manner as was described in detail in [9]. Tests were carried out for the layers with different structures, i.e. polycrystalline, amorphous and quasi-amorphous [10, 11, 12]. The layers for tests were obtained in "sandwich" planar laminar structure (the sequence of layers as follows: glass substrate-gold electrode-organic layer-aluminum electrode). The hole injecting electrode made of gold was used as a base, and outer aluminum electrode was used in two reasons: as a blocking holes, and as semitransparent for UV light. All the layers forming measuring cell were made by thermal evaporation in vacuum. The vaporization was made under pressure of the order of 10^{-5} Torr on glass plates maintained in temperature about 300 K. Structural examinations of obtained anthrone and anthrachinone layers were made using X – ray diffraction with use of an automatic diffractometer DAR. The diffraction studies were made in the 2θ range from 5° to 80° with measuring step 0,05°. Identical conditions of vacuum

thermal deposition for all tested samples protected the identity of the obtained structure of the layers for both studied materials.

In the presented paper we have trying to conduct a comparative study of mobility in layers of anthrone and anthrachinone with polycrystalline order. For these polycrystalline layers TOF measurements allowed to estimate the value of the mobility of holes in the layers of anthrone as a $(7\pm2)\cdot10^{-3}$ cm^2/Vs and for anthrachinone as a $(8\pm2)\cdot10^{-4}$ cm^2/Vs.

The difference of hole mobility values approximately in one order of magnitude for this two measured materials cannot be directly assigned to the crystal order of crystalline phase present in the both kinds of layers, because of the nearly identical crystal structures.

2.2. Computational methodology

The calculations were made with use TD-DFT (time dependent density functional theory) one of the most prominent methods for calculating exciting states, frequency – dependent response properties and photo absorption spectra of given molecule. All calculations were carried out with GAUSSIAN 09 program [13]. The structures of anthrachinone and anthrone were optimized using DFT at B3LYP (Becke three parameter (exchange), Lee Yang, and Parr) method using 6-311+g(d,p) basis set. The structures were considered completely optimized as stationary point was located and were confirmed by absence of imaginary frequencies. Taking the optimized geometric structures, the I.R, Raman, HOMO, LUMO and band gap calculations were performed with the same level of theory at ground state. UV–Vis spectra were simulated with TD-SCF using B3LYP/6-311+g(d,p).

The optimized geometric structures with electrostatic potential map of the anthrachinone and anthrone molecules in the ground state are shown in the Fig. 1 and both found to be planar, but the distribution of the atom charges in the anthrone molecule indicate the presence of dipole moment marked in the figure by the arrow.

The same molecules in the crystal are still planar but distances between the corresponding atoms in molecule are different. In the Table 1 and 2 (atoms in the bonds are signed as in the Fig. 1) we can see the comparison between bond lengths obtained from our calculations with TD-DFT for molecule with the findings obtained in the crystal phase with use of X-ray diffraction from the works of Srivastava [14] for anthrone (Table 2) and Murty [15] for anthrachinone (Table 1). The account of the overlapping of the molecules in the crystal structure is widely seen in the bond length C-O and for anthrone where unit shortening is 9.32% but for anthrachinone is small and equals only 0.32%.

The deformation of the corresponding bond lengths between carbons for both molecules in the crystal phase are different.
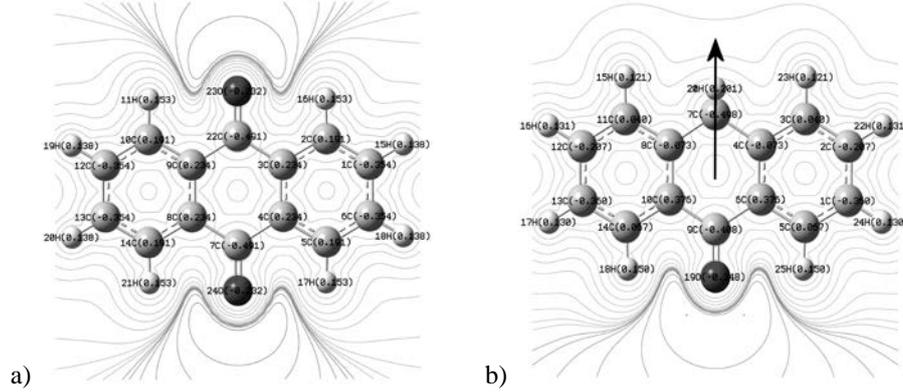

a)   b)

Fig. 1. Electrostatic potential map of anthrachinone a) and anthrone b). The plots are calculated with DFT B3LYP/6-311+g(d,p) at ground state

Table 1

Bond lengths for anthrachinone

bond	TD-DFT	X-ray analysis [15]	$\Delta = 10^3 \cdot (\{1\} - \{2\})$	$W = 10^{-2} \cdot (\{3\}/\{1\})$
	[Å] {1}	[Å] {2}	[Å] {3}	[%] {4}
24O – 7C	1.220	1.224	4	0,32
7C – 4C	1.492	1.478	14	0.94
4C – 3C	1.406	1.372	34	2.41
3C – 22C	1.492	1.478	14	0.94
22C – 23O	1.220	1.224	4	0.03
4C – 5C	1.398	1.391	7	0.05
5C – 6C	1.390	1.372	18	1.29
6C – 1C	1.398	1.410	12	0.86
1C – 2C	1.390	1.372	18	1.29
2C – 3C	1.398	1.391	7	0.05

Table 2

Bond lengths for anthrone

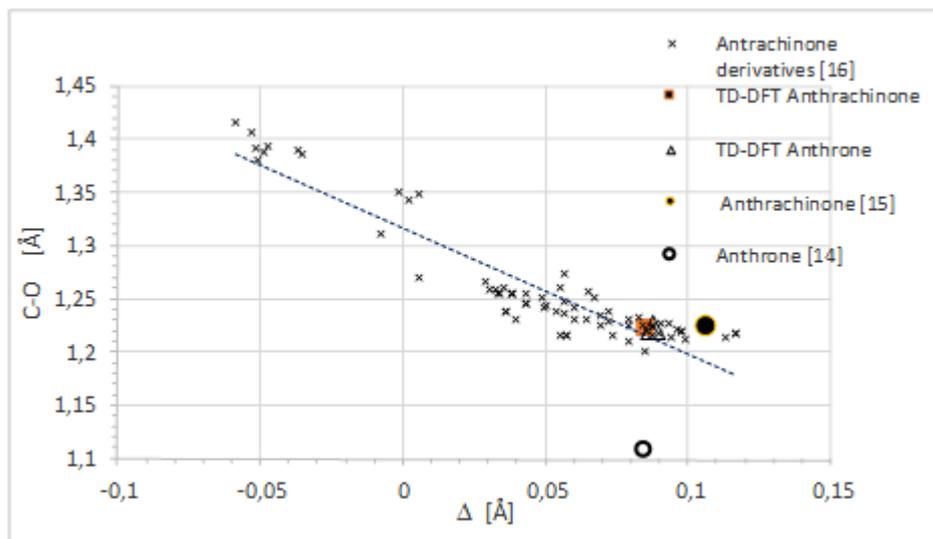| bond	TD-DFT	X-ray analysis [14]	$\Delta = 10^3 \cdot (\{1\} - \{2\})$	$W = 10^{-2} \cdot (\{3\}/\{1\})$
	[Å] {1}	[Å] {2}	[Å] {3}	[%] {4}
19O – 9C	1.223	1.109	114	9.32
9C – 6C	1.489	1.475	14	0.94
6C – 4C	1.402	1.391	11	0.78
4C – 7C	1.507	1.488	19	1.26
7C – 20H	1.097			
6C – 5C	1.404	1.389	15	1.07
5C – 1C	1.385	1.376	9	0.65
1C – 2C	1.399	1.364	35	2.50
2C – 3C	1.389	1.360	29	2.09
3C – 4C	1.401	1.412	11	0.79

Fig. 2. The experimental correlation of the dependence of *Δ* vs. C-O distances (x- data for 29 crystal structures of anthrachinone derivatives [16], ■ – TD-DFT anthrachinone, △ – TD-DFT anthrone, ● – anthrachinone from X-ray data [15], ○ – anthrone from X-ray data [14]).

Our TD-DFT calculations for anthrone and anthrachinone presented in the graph of Fig. 2 are in a good coincidence with data confirmed aromatic character of 29 crystal structures for anthrachinone derivatives. In this graph is presented dependence of $Δ = a\text{-}b$ (where a and b are the bond lengths, followingly for anthrone a = d(9C-6C), b = d(6C-4C) and for anthrachinone a = d(7C-4C), b = d(4C-3C)) on the C-O bond distance. The data point for crystalline anthrone [14] is distant from the main trend, showing the greater shortening and strengthening of the C-O bond what can be explained as high delocalization of π electrons in the central ring [16]. This observation is confirmed with the three dimensional graph of HOMO and HOMO-1 for anthrone (Fig. 3b, d) which is different to the centrosymmetric geometry of orbitals for anthrachinone (Fig. 3a, c). In the case of anthrone TD-DFT calculations show that the transition HOMO-LUMO is absent. For anthrone molecules the lowest singlet transition is seen in the Fig. 4b as the absorption gap in the UV spectrum ($λ$ = 294.64 nm, E = 4.208 eV). The calculated HOMO (hole acceptor orbital) of the anthrone molecules are seen to be substantially along C-O axis of conjugated system.
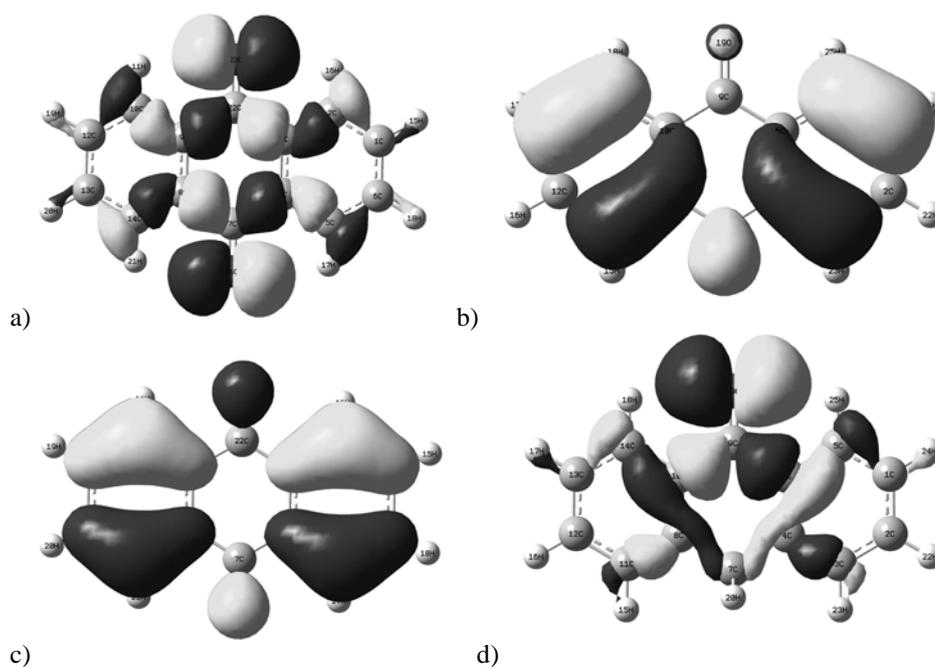
Fig. 3. Three dimensional pictures of HOMO and HOMO-1 of anthrachinone (a) and c) respectively) and anthrone (b) and d) respectively). The frontier orbitals plots are calculated with B3LYP/6-311+g(d,p) at ground state
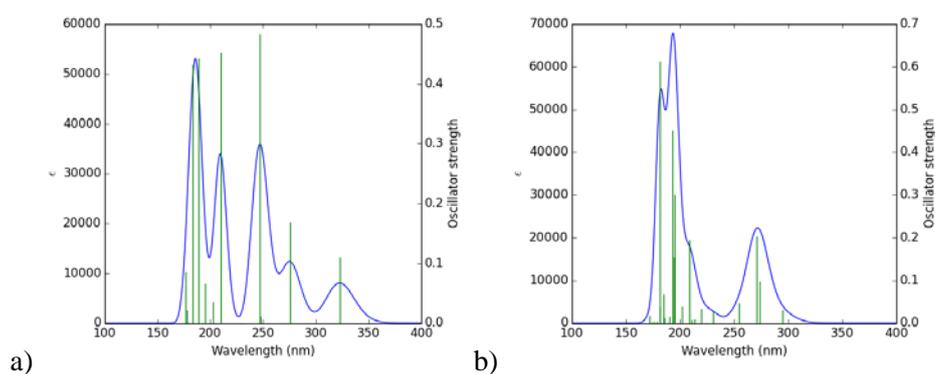

Fig. 4. The electronic spectra of anthrachinone a) and of anthrone b) calculated with B3LYP/6-311+g(d,p) at ground state

3. CONCLUSIONS

Based on the obtained results it could be built the conclusion, that for the increased mobility of anthrone layers is responsible the presence of the considerable value of dipole moment, in comparison to its lack for the anthrachinone layers. The presence of molecular dipole moment is responsible for different geometry of frontier orbitals in anthrone in comparison to anthrachinone. The shortening of the C-O bond in crystal phase is much greater for anthrone, which indicates an increasing aromaticity of the ring skeleton what can lead to greater conductivity. The unique nature of anthrone molecules and other non-centrosymmetrical aromatic ketones is seen in the increase of the dipole moment in the lowest triplet states which may be responsible for charge mobility. In the case of anthrone the lowest triplet state measured in microwave dielectric absorption is $\pi\pi^*$ [17], and from ours TD-DFT calculations the excitation energy is 3,066 eV. The shortening of C-O bond due to crystal forces for anthrone is 28,5 times greater than for anthrachinone. The disordered structure of a real anthrone crystal described with use of Ising coupling parameter [7] consists of the system of six independent infinite one-dimensional Ising chains. This situation with stacking disorder has the further consequence of intensify substantial disorder in the molecular orientation of the C-O group, registered in X-ray characterization as the increase of the crystal symmetry. Such a situation is responsible for mean trap distance correlated with mean disorder distance in *a* direction a range of 16 Å, and *b* direction 37±12 Å, and in the *c* direction 24±6 Å [7]. Additional disorder for anthrone in comparison to the anthrachinone for the temperatures higher than 150 K, i.e. for the temperatures when the hopping transport is dominant mechanism is responsible for additive concentration of shallow traps in the case of anthrone layers in comparison with anthrachinone ones.

When neutral organic molecule is charged during hole transport, it forms cationic open -shell electronic configuration which corresponds to process of

$$M \rightarrow M^+ + e^-. \tag{1}$$

The energy change connected with this charge transfer is called the internal reorganization energy (λ^{int}). Electronic polarization of surrounding molecules is connected with external reorganization energy (λ^{ext}).

The total reorganization energy between *i* and *j* molecule may be described as a sum of internal and external terms

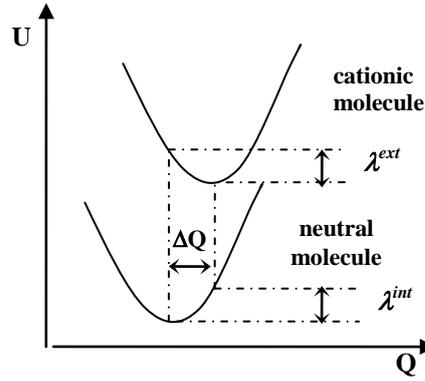$$\lambda_{ij} = \lambda_{ij}^{\text{int}} + \lambda_{ij}^{ext} \tag{2}$$

Fig. 5. Schematic representation of the potential energy surfaces of the neutral and cationic molecules. (Q – reaction coordinate, U – potential energy)

In the high temperature limit, the transfer rate for a charge to hop from a site *i* to a final site *j* is [18]

$$k_{ij} = \frac{2\pi}{\eta} \frac{J_{ij}^2}{\sqrt{4\pi\lambda_{ij}k_BT}} \exp\left[-\frac{\left(\Delta E_{ij} - \lambda_{ij}\right)^2}{4\lambda_{i\alpha}k_BT}\right], \tag{3}$$

where: T is temperature, k_B is the Boltzmann constant, ΔE_{ij} – is difference of electron energy between the initial and final molecular sites, η – is the reduced Planck constant, J_{ij} – is a transfer integral describing electron transfer from molecule *i* to molecule *j*.

The theoretical description of the conductivity of the molecular systems needs the understanding the fact that nuclear dynamics is much slower than the dynamics of charge carriers and the fact that electronic coupling is weak. This fact enables to divide the whole system to the subsystems, and to present the Hamiltonian operator describing the whole system as a sum of terms.

For molecular systems coupling calculations commonly are made using density functional theory (DFT). Applying the self-consistent formalism to construct the Kohn-Sham-Fock operator for dimer interactions with assumption that HOMO and HOMO-1 of the dimer results only from the interaction of the monomers HOMO, the secular equation for dimer molecular orbitals and the corresponding dimer orbital energies will be in the form

$$\boldsymbol{HC}\text{-}\boldsymbol{ESC} = 0, \tag{4}$$

where: $\boldsymbol{H}$ and $\boldsymbol{S}$ are the Hamiltonian and overlapping matrices of the system, and $\boldsymbol{C}$ and $\boldsymbol{E}$ are the Kohn-Sham molecular orbital coefficients and eigenenergies of the non-interacting dimer, respectively.

The above quantities are in the form

$$H = \begin{pmatrix} E_1 & J_{12} \\ J_{12} & E_2 \end{pmatrix}, \tag{5}$$

and

$$S = \begin{pmatrix} 1 & S_{12} \\ S_{12} & 1 \end{pmatrix}, \tag{6}$$

where the matrix elements are defined as

$$E_i = \left\langle \Psi_i \middle| \hat{H} \middle| \Psi_i \right\rangle, \tag{7}$$

$$J_{ij} = \left\langle \Psi_i \middle| \hat{H} \middle| \Psi_j \right\rangle, \tag{8}$$

$$S_{ij} = \left\langle \Psi_i \middle| \Psi_j \right\rangle. \tag{9}$$

Transfer integral (8) describes electron transfer from molecule i to molecule j with overlapping energy J_{ij}.

Dipole-dipole interactions energy between the dipole ds_1 in the centre of the coordinate system having direction s_1 in the field originated from the network of point dipoles with directions s_n is shown below in the form of the sum of interactions with all other dipoles [19]

$$\delta J_{1\alpha} = \frac{d^2}{2} \sum_{n=2}^{\infty} \left[\frac{s_1 s_n}{|r_{1n}|^3} - \frac{3(s_1 r_{1n})(s_n r_{1n})}{|r_{1n}|^5} \right], \tag{10}$$

where: s_n and r_n are vectors, r_{1n} is a position of n-th dipole, α-sign a manifold of the network of point dipoles. This energy for anthrachinone, with the molecules without significant natural dipole moment is in the order of 10^{-5}-10^{-6} eV, that is much less than the van der Waals potential energy (estimated in the range of 10^{-3}-$7 \cdot 10^{-2}$ eV), but for anthrone molecules with a significant natural dipole moment of 3,5 D the energy of dipole-dipole interaction can be as much as 10^{-2}-10^{-3} eV, the value comparable to the van der Waals potential. These additional dipole-dipole energies present for anthrone structures can lead to broadening of the bands for anthrone in the condensed form and to the enlarging overlapping of the wave functions what is favourable to enhancing conduction of the charge carriers via localized states.

For both molecular compounds in condensed state experimental values of the mobility in the room temperature are below 10^{-2} cm^2/Vs indicate hopping transport with very similar value of the activation energy for both compounds. Therefore, for anthrone, with molecule possessing a natural dipole moment, the

mobility of holes in the condensed state is almost one order of magnitude greater than that measured for anthrachinone and this fact can be connected with the higher value of transfer rates connected with the greater density of traps for anthrone which is connected with disorder dependent on its molecular dipole moment.

Acknowledgements

REFERENCES

[1] Di **C**., Zhang F., Zhu D. 2013. Multifunctional Integration of Organic Field-Effect Transistors (OFETs): Advances and Perspectives. Adv. Mater. 25: 313-330.

[2] Andersson M.R., Berggren M., Inganäs O., Gustafsson G., Gustafsson-Carlberg J.C., Selse D., Hjertberg T., Wennerström O. 1995. Electroluminescence from Substituted Poly(tiophenes): From Blue to Near-Infrared. Macromolecules 28: 7525-7529.

[3] Harris J. W. 1965. Mixed anthrone-anthraquinone crystals. Nature. 206: 1038.

[4] Srivastava S.N. 1962. Crystal structure of anthrone. Zeitschrift für Kristallographie. 117: 386-398.

[5] Angyal C.L., Le Fevre R.J.W. 1950. The polarities of enols. J. Chem. Soc. 106: 562-564.

[6] Srivastava S.N. 1961. Diffuse layers in anthrone photographs. Acta Cryst. 14:796.

[7] Reynolds P. A. 1975. A calculation of the molecular orientational disorder in crystalline anthrone. Acta Cryst. A 31: 80-83.

[8] Ong B.K., Woon K.L., Ariffin A. 2014. Evaluation of various density functionals for predicting the electrophosphorescent host HOMO, LUMO and triplet energies. Synth. Met. 195: 54-60.

[9] Kania S., Kondrasiuk J., Bąk G.W. 2004. Influence of ambient atmosphere on charge transport in polycrystalline thin films of three simple aromatic hydrocarbons. Eur. Phys. J. E 15: 439-442.

[10] Kania S. 2009. Hole drift mobility in anthrone layers. Visnyk Lviv Univ. Ser. Physics 43: 49-56

[11] Kania S. 2013. Hole drift mobility for different structures of anthrone and anthrachinone layers. Sci. Bull. Tech. Univ. of Łódź, Physics 34: 19-25.

[12] Kania S. 2014. Hole drift mobility of anthrone and anthrachinone layers with different structures. Sci. Bull. Techn. Univ. Lodz, Physics, 35: 17-24.

[13] Gaussian 09, Revision A.02, Frisch M.J., Trucks G.W., Schlegel H.B., Scuseria G.E., Robb M.A., Cheeseman J.R., Scalmani G., Barone V., Mennucci B., Petersson G.A., Nakatsuji H., Caricato M., Li X.,. Hratchian H.P, Izmaylov A.F., Bloino J., Zheng G., Sonnenberg J.L., Hada M., Ehara M., Toyota K., Fukuda R., Hasegawa J., Ishida M., Nakajima T., Honda Y., Kitao O., Nakai H., Vreven T., Montgomery J.A. Jr., Peralta J.E., Ogliaro F., Bearpark M., Heyd J.J., Brothers E., Kudin K.N., Staroverov V.N., Kobayashi R., Normand J., Raghavachari K., Rendell A., Burant J.C., Iyengar S.S., Tomasi J., Cossi M., Rega N., Millam J.M., Klene M., Knox J.E., Cross J.B., Bakken V., Adamo C., Jaramillo J., Gomperts R., Stratmann R.E., Yazyev O., Austin A.J., Cammi R., Pomelli C., Ochterski J.W., Martin R.L., Morokuma K., Zakrzewski V.G., Voth G.A., Salvador P., Dannenberg J.J., Dapprich S., Daniels A.D., Farkas O., Foresman J.B., Ortiz J.V., Cioslowski J., Fox D.J. 2009. Wallingford CT: Gaussian, Inc.

[14] Srivastava S.N. 1964. Three-Dimentional refinement of the structure of anthrone. Acta Cryst. 17: 851-856.

[15] Murty B.V.R.1960. Refinement of the structure of anthraquinone. Zeitschrift für Kristallographie 113: 445-465.

[16] Kožíšek J., Breza M., Ulický L. 1993. Aromatic character of anthraquinone derivatives. Chem. Papers 47: 34-37.

[17] Shimamori H., Houdo K., Uegaito H., Nakatani Y., Uchida K. 1989. Detection of Excited Triplet states of Aromatic Ketones and Determinaton of Their Dipole Moments by the Time-Resolved Microwave dielectric Absorption Technique. Chem. Soc. Jap. 8: 1379-1385.

[18] Rühle V., Lukyanov A., Falk M., Schrader M., Vehoff T., Kirkpatrick J., Baumeier B., Andrienko D. 2011. Microscopic Simulations of Charge Transport in Disordered Organic Semiconductors. J. Chem. Theory Comput. 7: 3335-3345.

[19] Kitaigorodskii A.J. 1973. Molecular Crystals and Molecules, New York: Acad. Press.

WPŁYW MOMENTU DIPOLOWEGO
NA PRZEWODNICTWO DZIUR W WARSTWACH
POLIKRYSTALICZNEGO ANTRONU
I ANTRACHINONU

Streszczenie

Dokonano złożonej analizy, wykorzystując metody kwantowej mechaniki molekularnej dla zbadania wpływu obecności momentu dipolowego molekuły antronu i molekuły antrachinonu na ruchliwość ładunków w warstwach polikrystalicznych zbudowanych z takich molekuł. Źródłem zróżnicowania uzyskiwanych w pomiarze wartości ruchliwości wydaje się być w pierwszym rzędzie różnica geometrii zewnętrznych orbitali molekularnych dla obu badanych molekuł, a nie różnica tkwiąca w uporządkowaniu krystalicznym tychże molekuł, która dla obu jest bardzo podobna, gdyż oba związki krystalizują w identycznej strukturze $C_{2h}^5(P2_1/a)$.